Accepted Manuscript

Geological Society, London, Special Publications

Cross-Basin Mo and U Analysis of the Upper Mississippian Bowland Shale UK

J. Walker, J. F. Emmings, S. Acikalin, S. L. Flynn, C. Van der Land, M. Jones, C. H. Vane, J. A. I. Hennissen, E. Hough, T. Wagner & L. Craddock

DOI: https://doi.org/10.1144/SP534-2022-231

To access the most recent version of this article, please click the DOI URL in the line above. When citing this article please include the above DOI.

Received 1 August 2022
Revised 18 May 2023
Accepted 21 May 2023

Cross-Basin Mo and U Analysis of the Upper Mississippian Bowland Shale UK

J. Walker[1*], J. F. Emmings[2], S. Acikalin[3], S. L. Flynn[3], C. Van der Land[3], M. Jones[3], C. H. Vane[4], J. A. I. Hennissen[4], E. Hough[4], T. Wagner[5], L. Craddock[6]

[1]Edge Hill University, Ormskirk, Lancashire, L39 4QP

[2]CGG, Tyn Y Coed, Llanrhos, Llandudno, LL30 1SA

[3]School of Natural and Environmental Sciences, Newcastle University, Newcastle upon Tyne, Tyne & Wear, NE1 7RU, UK

[4]British Geological Survey, Keyworth, Nottingham NG12 5GG

[5]The Lyell Centre, Heriot-Watt University, EH14 4AP

[6]Cuadrilla Resources Ltd, Manchester Business Park, 3000 Aviator Way, Wythenshawe, Manchester, M22 5TG

*Correspondence jack.walker12345@hotmail.co.uk

Abstract

The Bowland sub-basin is a target for hydrocarbon exploration but to a large extent it remains unexplored. To determine the economic potential of the Bowland sub-basin, it is important to identify the oceanographic processes involved in the deposition of the Bowland Shale Formation in the Late Mississippian (*ca*. 330 Ma). Palaeoceanographic processes are known to be a major control on the development of hydrocarbon source rocks. This study investigates core (Preese Hall-1 and Becconsall-1Z) materials from the Upper Bowland Shale, and compares to previously published data (outcrop Hind Clough), all from the Bowland sub-basin, Lancashire, UK. The sedimentology and geochemistry of this formation was determined via a multi-technique approach including x-ray fluorescence (XRF), sedimentology, gamma ray spectra, x-ray diffraction (XRD) and RockEval(6)™ pyrolysis. Key trace metal abundances and enrichment factors were used to assess sediment provenance and to determine the bottom water redox conditions during the deposition of the Upper Bowland Shale. Our results support interpretations that contemporaneous anoxia developed in bottom waters in at least three sites in the Bowland sub-basin. In a comparison with the Fort Worth Basin (Barnett Shale, USA), the Bowland sub-basin was apparently less restricted and deposited under a much higher mean sediment accumulation rate compared to the Fort Worth Basin. Knowledge from this study improves future resource estimates of the Bowland Shale Formation, and challenges the early assumptions that the Barnett Shale is an analogue to the Bowland Shale.

The Late Mississippian-Early Pennsylvanian Bowland Shale Formation in England is an exploration target for hydrocarbon reserves, focussing on shale gas (Andrews 2013; Fearn 2022). In 2022, shale gas exploration in the Bowland Shale Formation had become the focus of political debate on UK hydraulic fracturing legislation after a moratorium was lifted in September, only to be re-instated in November (Baptie *et al.* 2022). These circumstances continue to limit the volume of core material and data available for research on the Bowland Shale Formation. Open access production data from the Bowland Shale are limited. Thus, the size of the hydrocarbon resource in the Bowland Shale Formation is still a contentious topic (Andrews 2013; Whitelaw *et al.* 2019; Lodhia *et al.* 2023). For example, resource estimations by Andrews (2013) relied on data from the Barnett Shale Formation, USA. Andrews (2013) used the Barnett Shale Formation as an analogue for the Bowland Shale because (1) data from the Bowland Shale were lacking, and; (2) because it shared "close similarities" with the Bowland Shale Formation in terms of total organic carbon and pyrolyzable organic matter content. Our study aims to contribute to our evolving understanding of the environmental conditions during deposition of the Bowland Shale in the Bowland sub-basin (Craven Basin), with implications for understanding the relevance of the Barnett Shale as an analogue to the Bowland Shale.

Here, we use high resolution inorganic and organic geochemistry to reconstruct the palaeoceanographic and palaeoredox conditions during deposition of the Upper Bowland Shale in two wells in the distal Bowland sub-basin. We conducted x-ray fluorescence (XRF) sedimentology, biostratigraphy, gamma ray spectroscopy, RockEval(6)™ pyrolysis and x-ray diffraction (XRD) on core materials. We link these new observations to previously published findings (see Emmings *et al.*, 2020 and references therein) to develop an interpretation of the Upper Bowland Shale across the Bowland sub-basin. We focus on elemental proxies for sediment provenance (TiO_2, Zr and to some degree Ni) and palaeoredox conditions (Mo and U). Our interpretations are limited to the key uncertainties regarding the palaeomorphology and palaeobathymetry of this sub-basin, particularly regarding the locations and extent of this sub-basin's seabed topography (Clarke *et al.* 2018; de Jonge-Anderson *et al.* 2020; Emmings *et al.* 2020a). Here were focus on the Upper Bowland Shale in the Becconsall-1Z borehole (53 41' 58.6291" N, 2 53' 57.3813; BGS reference number SD42SW/11) and Preese Hall-1 borehole (53 49' 19.006" N; 2 56'56.576"; BGS reference number SD33NE/38), alongside the previously analysed outcrop Hind Clough located in a more proximal location (53 58' 25.4"N 2 32' 37.6"; see Emmings *et al.*, 2020a and references therein). Both cores and the outcrop section include time-equivalent beds as constrained by the presence of the ammonoid index fossil *Tumulites pseudobilingue* ($E_{1b}2$) (Brandon *et al.* 1998; Clarke *et al.* 2018).

Geological History

Craven Basin Structure

The Craven Basin (including the Bowland sub-basin) formed as a result of normal fault reactivation of Caledonian lineaments during the closure of the Rheic Ocean in the late Devonian (Fraser and Gawthorpe 2003; Timmerman *et al.* 2009; Davies *et al.* 2012; Clarke *et al.* 2018), linked to Mississippian crustal extension (Leeder 1988; Corfield *et al.* 1996). The faulted Bowland High separates the Bowland sub-basin from the adjacent Lancaster Fells sub-basin towards the north-west, both within the larger Craven Basin (see Emmings *et al.* 2020a and references therein). Fault systems ultimately bound the Craven Basin from the Southern Lake District High and Askrigg-

Bowland High to the north and Central Pennine High to the south east (Gawthorpe 1987; Hough *et al.* 2014; **Fig. 1**). The Craven Fault System and Pendle Lineament bound the sub-basin in the north and southeast, respectively (Leeder 1988; Fraser and Gawthorpe 1990; Worthington and Walsh 2011) and the Variscan orogenic compression promoted folding (Arthurton 1984; Arthurton *et al.* 1988; Corfield *et al.* 1996).

The Craven Basin was inverted during the Pennsylvanian Variscan orogeny (*ca.* 323.2 Ma) (Arthurton 1984; Gawthorpe 1987; Pharaoh *et al.* 2019). This resulted in a set of north-east to south-west trending thrust-folds, monoclines and folds defined collectively as the Ribblesdale Fold Belt (Arthurton 1984; Gawthorpe 1987; Pharaoh *et al.* 2019). Maximum burial was attained during the Late Cretaceous (Andrews 2013; Clarke *et al.* 2018; Pearson and Russell 2020). RockEval T_{max} and laser Raman analyses of vitrinite from Hind Clough suggest most samples are immature to early oil mature (Henry *et al.* 2018; Emmings *et al.* 2020b). RockEval T_{max} reported by Clarke *et al.* (2018) suggests that subsurface cores from the Bowland Shale Formation (including Preese Hall-1 and Becconsall-1Z) have been buried into the upper oil (c. 450 °C) to dry gas (>470 °C) windows.

Becconsall-1Z is located towards the southern margin of the sub-basin, while Preese Hall-1 is near to the central part (**Fig. 1**). The Hind Clough section is located northeast of Becconsall-1Z and Preese Hall-1, closer to the primary source of detrital sediment delivered via the Pendle Delta system (e.g., Clarke *et al.* 2018). Thus, the selected locations in this study span a proximal-distal transect across the Bowland sub-basin (**Fig. 2**).

Stratigraphy

Biostratigraphy is used to correlate key stratigraphic boundaries in the Upper Bowland Shale (e.g., Waters *et al*. 2009). Macrofaunal body fossils, particularly ammonoids, are used to construct a high-resolution biostratigraphic framework (Ramsbottom and Saunders 1985). However, the macrofaunal index fossils can be difficult to recognise in core (Riley 1993; Waters *et al.* 2009; Clarke *et al.* 2018). The macrofossils are used to identify the key stratigraphic boundaries (e.g., Waters *et al*. 2009), including glacio-eustatic highstands (Dunham and Wilson 1985; Read *et al.* 1991; Bhattacharya 1993; Church and Gawthorpe 1994; Martinsen *et al.* 1995; Davies and McLean 1996; Hampson *et al.* 1997; Isbell *et al.* 2003). Carbonate-bearing, bioclastic mudstone packages bearing ammonoid index taxa are colloquially termed 'marine bands' because they likely reflect deposition during periods of glacioeustatic high stands (Ramsbottom 1977; Ramsbottom 1979; Holdsworth and Collinson 1988; Martinsen 1990; Waters and Condon 2012).

The relationship between geochemistry, deposition and post-deposition of marine bands is debated because the geochemical signals are not consistent between or within formations (Ramsbottom 1979; Davies and Elliott 1996; Davies and McLean 1996; Clarke *et al.* 2018). For example, marine bands can exhibit a sharp increase in total organic carbon (TOC) and/or gamma ray spectra intensity (Davies and Elliott 1996; Davies and McLean 1996; Clarke *et al.* 2018; Emmings *et al.* 2020a), but these characteristics are not ubiquitous (Clarke *et al.* 2018).

Nonetheless, the marine bands in the Bowland Shale Formation are important because they are one of the few ways to resolve the stratigraphy where laterally persistent lithological marker beds are sparse. Whilst the ammonoids do not occur throughout the cores and outcrop, the macrofauna have a higher temporal resolution than miospores (see Hird *et al.* 2012a; 2012b; Clarke *et al.* 2018;

Hennissen *et al.* 2017; 2020). In this current study, we use the term marine band to describe a macrofauna, ammonoid-bearing sedimentary package within a broader fourth-order stratigraphic cycle (e.g., Ramsbottom 1977; Ramsbottom 1979; Martinsen 1990; Martinsen *et al.* 1995; Waters and Condon 2012; Gross *et al.* 2015). The current study is based upon a correlative framework afforded by recognition of the $E_{1b}2$ marine band, bounding the $E_{1a}1$ and $E_{1b}2$ biozones.

The $E_{1b}2$ marine band is defined by the presence of the ammonoid index taxon *Tumulites pseudobilingue* (Brandon 1998; Clarke *et al*. 2018), recognised in Becconsall-1Z (grid ref: 4229776.44, 340636.02; BGS reference number SD42SW/11) and Preese Hall-1 (grid ref: 436627.491, 337531.684; BGS reference number SD33NE/38) (**Fig. 1**; also in Clarke *et al.* 2018). The $E_{1b}2$ marine band is also identified in outcrop at Hind Clough (grid ref: 364430, 453210, British National Grid projection) (Brandon *et al.* 1998). In Becconsall-1Z, the base of the Upper Bowland Shale is proven by the marine band $E_{1a}1$ coupled to sharp increases in the gamma ray response (Clarke *et al.* 2018). At Preese Hall-1, the base of the Bowland Shale Formation has not been cored (**Fig. 1**) and overall the stratigraphy at Preese Hall-1 is less certain (Clarke *et al.* 2018). Regionally, the top of the Upper Bowland Shale is marked by the base of the lowermost sandstone of the Millstone Grit Group, which in some areas is a conformable boundary, and an erosional boundary at others (Earp *et al.* 1961; Fewtrell *et al.* 1981; Waters *et al.* 2009).

Sedimentology, palaeoenvironment and palaeoredox conditions

During the Mississippian, Britain was positioned south of the equator at ~5-10° S (Scotese and McKerrow 1990; Aitkenhead 1992; Cocks and Torsvik 2006; Woodcock and Strachan 2009). The Upper Bowland Shale was deposited in the Bowland sub-basin via density flows and hemipelagic sedimentation (Bisat 1924; Aitkenhead 1992; Smith *et al.* 2005; Andrews 2013; Clarke *et al.* 2018; Emmings *et al.* 2020b). Turbidity currents and hybrid flows were likely an important mechanism for transport and deposition of sediment in the proximal part of the basin (Emmings *et al.* 2020a; 2020b). Previous sedimentological studies have used flow direction indicators to suggest primary sedimentation is sourced from the north, associated with the prograding Pendle delta system linked to the overlying Pendleside Sandstone Member of the Millstone Grit Group (Bisat 1924; Walker 1966; Collinson 1968, 1969; Ramsbottom *et al.* 1978; Collinson *et al.* 1988; Holdsworth and Collinson 1988; Fraser and Gawthorpe 2003; Kane 2010).

Methodology

Biostratigraphy and Marine Band Identification

At Becconsall-1Z, the Upper Bowland Shale is 85 m thick (Hird *et al.* 2012a). Here, the base of marine band $E_{1a}1$, and therefore the base of this unit, is found at 2219.86 m (true vertical depth). The top of this unit at Becconsall-1Z is at 2135.10 m depth. In the cored section of this well, *Tumulites pseudobilingue* was identified between 2140.90 m to 2142.59 m and estimated to be 1.69 m thick (Hird *et al.* 2012a; Clarke *et al.* 2018). Therefore, the thickness of the Becconsall-1Z studied succession between the base of $E_{1a}1$ and top of $E_{1b}2$ was 78.96 m. At Preese Hall-1, the Upper Bowland Shale is 512 m thick (Hird *et al.* 2012b; Clarke *et al*. 2018) ranging from *ca.* 2504 to 1992 m (true vertical depth). At Preese Hall-1, *Tumulites pseudobilingue* index fauna were identified between 2081.75 to 2081.81 m depths (Hird *et al.* 2012b). Therefore, at Preese Hall-1, the minimum thickness of the $E_{1b}2$ ammonoid phase was 6 cm. Emmings *et al.* (2020a) showed that the thickness

of the Upper Bowland Shale is *ca.* 102 m thick at Hind Clough. The thickness between the unit's base and $E_{1b}2$ is *ca.* 63 m (Emmings *et al.* 2020a).

The Upper Bowland Shale was logged and sampled at *ca.* 1 m intervals, fractures were avoided, and sample intervals were kept as evenly spaced as possible. 20 g samples were collected and thoroughly cleaned using a wire brush, and a mixture of dichloromethane and methanol to remove contaminants. Samples were crushed to a homogenised powder and sub-sampled. Data collected from cuttings and gamma ray spectroscopy have different sample intervals to RockEval(6)™ and XRF data. Ratio errors consider the magnitude of propagated error (Holmes and Buhr 2007).

X-ray Fluorescence

Fifty-six samples from Becconsall-1Z (26) and Preese Hall-1 (30) were crushed and milled to a fine powder, and sub-samples (4 g) were then packed into the bottom of a sample cup for x-ray fluorescence (XRF) analysis. The samples were analysed using a SPECTROSCOUT ED-XRF at Chemostrat Ltd. Reference standards were analysed every 10 samples to correct for machine drift. Six control samples were run along with the other samples for error assessment. Pressed powder and fused bead samples from Hind Clough were analysed using a PANalytical Axios WD-XRF system (Malvern PANalytical, Malvern, UK; see Emmings *et al.* 2020a and references therein). Here we focus on the elements which proxy for sediment provenance (TiO_2, Zr and potentially Ni) and palaeoredox conditions (Mo and U). Element enrichment factors are normalised to Post-Archaean Average Shale (PAAS; see Emmings *et al.*, this volume for details).

Rock-Eval Pyrolysis

The same samples as those used for XRF analysis were also sub-sampled for pyrolysis analysis. All sub-samples were crushed, homogenised and sieved (250 µm) and analysed using a Rock-Eval(6)™ analyser (at the British Geological Survey) configured in standard mode (Behar *et al.* 2001; Słowakiewicz *et al.* 2015; Newell *et al.* 2016). Rock-Eval(6)™ pyrolysis was prioritised over HAWK (Jarvie *et al.* 2015) and high pressure water pyrolysis (Whitelaw *et al.* 2019) to more reliably compare results with previous Bowland sub-basin studies (e.g., Emmings *et al.* 2017; Emmings *et al.* 2020a). Dry sub-samples (60 mg) were heated and held at 300 °C for 3 minutes and then heated to 650 °C. Released hydrocarbons were measured using a flame ionization detector (FID). The T_{max} was calculated from the T_{peak} S2 – 37 °C (Behar *et al.* 2001). Instrument quality was checked every 10 samples against the accepted values of the Institut Français du Pétrole (IFP) standard. 6 control samples and the IFP reported values were used for error assessment.

Additionally, we estimate original TOC (TOC_0) from the start of hydrocarbon generation using the formula TOC_0 = TOC/(1-0.363), after Jarvie *et al.* (2003) and Montgomery *et al.* (2006). This formula assumes a Barnett Shale immature precursor organic composition and implies a reduction in the original TOC by *ca.* 36%. This value is within typical ranges of TOC reduction during maturation, calculated by Hart and Hofmann (2022). However, we note Hennissen et al. (this volume) and Emmings et al. (this volume) derived the equation TOC_0 = 1.16TOC-0.16 in the oil-to-gas mature Bowland Shale in the adjacent Blacon Basin (calibrated using palynofacies analysis). This latter formula implies only a small TOC reduction of 16% during thermal maturation, and is based upon original HI (HI_o) contents less than *ca.* 500 (see Hennissen et al., 2017; Hart and Hofmann, 2022). This is consistent with a mixture of type II/III organic matter associated with quantitative refractory (non-pyrolysable) organic matter in the Bowland Shale, as supported by palynological observations (e.g.,

Hennissen et al., 2017; Emmings et al., 2019). Additionally, the section at Hind Clough is immature to early oil mature, and potentially contains a greater fraction of terrestrial (gas prone) organic matter due to proximity to the Pendle delta system (Emmings *et al.* 2020a, 2020b). Thus, TOC_0 estimation that assumes a 36% reduction in TOC during thermal maturation likely represents an extreme upper bound estimate, particularly for Hind Clough. The *true* TOC_0 likely resides on a mixing line between the present-day TOC and our TOC_0 upper bound estimate.

Gamma

The gamma ray data derive from digitized open access well reports (Hird *et al.* 2012a; Hird *et al.* 2012b) through the entire Upper Bowland Shale in each well (**Fig. 2**). Synthetic gamma ray for the Hind Clough samples was calculated using the concentrations of U, Th and K (see Ellis and Singer 2007; see also Emmings *et al*. this volume).

Cuttings

XRD mineralogical data derive from the Becconsall-1Z and Preese Hall-1 well reports. Fine fraction XRD had been previously used to analyse these cuttings. All cuttings had been previously crushed (c. 2 μm) and analysed using a Cu x-ray tube with a Siemens D500™ instrument, between 3 and 70° 2θ. Peak identification used PDF-4 Minerals database 2009 and peaks were quantified using Jade 9™ software (Rietveld analyses).

All geochemical data from Becconsall-1Z and Preese Hall-1 are available via the DOI: 10.25405/data.ncl.12102492 (Newcastle University).

Results

X-ray Diffraction (Cuttings)

The percentage of quartz minerals at Preese Hall-1 ranges from 22 to 79 % with an average of 58 ±13 %. These relative abundances of quartz are similar in Becconsall-1Z, where the average quartz content is 55 ±10 % and ranges from 35 to 68 %. The clay mineral content in Preese Hall-1 ranges from 0 to 56 %, with an average of 23 ±12 %, compared to 18 to 59 % and average of 38 ±12 % at Becconsall-1Z. The carbonate abundances exhibit an average of 19 ±19 % and 8 ±7 % at Preese Hall-1 and Becconsall-1Z respectively. Becconsall-1Z carbonate content ranges from 2 to 31 %. Relative carbonate content at Preese Hall-1 range from 0 to 79 %.

Gamma Ray Spectroscopy

Gamma ray data from Becconsall-1Z ranged from 27 to 239 (API) with an average of 112 ±46. The Upper Bowland Shale at Preese Hall-1 exhibits an average gamma ray of 80 ±25 and range from 25 to 179 (**Table 1, Fig. 2)**. At Hind Clough, synthetic gamma ray values exhibit a greater average value, compared to the two cores, of 165 ±52 (ranging from 58 to 285). For all three sites, gamma ray values in the Upper Bowland Shale range between 25 and 285.

X-ray Fluorescence

Cross-plots of the concentrations of Zr and TiO_2 indicate that Beconsall-1Z, Preese Hall-1 and Hind Clough are within or near to the border of the Felsic Igneous Provenance Zone (**Fig. 3a**; Hayashi *et al.* 1997). Four samples within the Intermediate Igneous Provenance Zone are from Preese Hall-1. Each site shows a positive correlation of TiO_2 and Zr, but their strengths of correlation vary. At Hind

Clough and Preese Hall-1, concentrations of Zr and TiO_2 are weakly correlated (R^2 values of 0.44 and 0.34 respectively), whereas Zr and TiO_2 at Becconsall-1Z are strongly correlated (R^2 was 0.93). The range of Zr concentrations differ within each location, with the greatest range of Zr at Hind Clough (29.1 to 129.6 ppm) and Preese Hall-1 (40.9 to 133.1 ppm). Becconsall-1Z shows the most limited range of Zr values (36.2 to 99.8 ppm).

The average TiO_2 content is lowest at Hind Clough (0.14 %), where Zr ranges from 0.05 to 0.31 %. However, average TiO_2 concentrations are largest at Preese Hall-1 (0.46 %), and this location also exhibits the largest range (0.15 to 0.69 %) compared to the other sites. The Becconsall-1Z section has an average TiO_2 content of 0.38 % and a range of 0.18 to 0.60 %. For each site, the R^2 value for Ni and TiO_2 concentration cross-plots were less than 0.5.

Preese Hall-1 Ni concentrations range from 12.6 ppm to 148.1 ppm, where the average values are lowest of the three sites (61.5 ppm). The widest range of Ni values and highest average are at Hind Clough 9.8 to 399.4 ppm and 108.6 ppm, respectively. Furthermore, Ni values at Becconsall-1Z exhibit an average of 77.5 ppm where the range is smallest, from 57.1 to 121.1 ppm. Biplots of Ni and TiO_2 (cf. Floyd *et al.* 1989; **Fig. 3b**) shows all three locations exhibit relatively low TiO_2 and wide-ranging Ni concentrations. All samples plot on a series of mixing lines bounded by sedimentary maturity and an origin close to the Felsic Zone. None of the sites plot within or near to the Mafic Zone Magmatogenic Graywackes (thresholds previously outlined by Floyd *et al.* 1989).

U and Mo enrichment factors (EF) were compared to Zr, TiO_2 and TOC at the three locations (**Fig. 4)**. U-EF exceed 0.8 at all sites; Preese Hall-1Z (6.1 U-EF), Becconsall-1Z (8.8 U-EF) and Hind Clough (8.5 U-EF). The range of values is largest at Hind Clough (4.2 to 20.6) and smallest at Becconsall-1Z (4.5 to 16.3). U-EF ranges from 0.8 to 16.6 at Preese Hall-1. All Mo-EF values are greater than 2.0 at all three sites, with the largest average values at Hind Clough (77.9) and smallest at Preese Hall-1 (37.6). The average Mo-EF is 47.1 at Becconsall-1Z. The ranges of Mo-EF differ across the two cores. Becconsall-1Z Mo-EF values range from 14.9 to 79.4. At Preese Hall-1 and Hind Clough, the Mo-EF values range from 2.0 to 83.8 and 5.0 to 156.9, respectively.

Principal Component Analysis (PCA) was used to assess correlations between the selected elements, together with the correlation coefficient R^2. Zr is not correlated with U-EF or Mo-EF at any of the three sites (**Fig. 4**); R^2 correlation coefficients are less than 0.5 in all cases. **Fig. 4** shows the relationship between TiO_2 versus U-EF and Mo-EF. In all these sites, the R^2 value is less than 0.5 (showing weak to no correlations). To understand the relationship of organic matter to U-EF and Mo-EF, we plotted TOC against each of these two inorganic proxies. The TOC values do not correlate with either proxy (R^2 values less than 0.5), except for TOC and U-EF relationships in Becconsall-1Z where there is moderate correlation (R^2 value of 0.7) between TOC and U-EF.

A biplot of the first two principal components provides a means to visualize new variables (PC1, PC2) which describe the maximum variance in the dataset (**Fig. 5)**. At Preese Hall-1, Fe, Mo, Ni, TiO_2, Al, K and Zr are broadly correlated with PC1 and are inversely correlated with Ca. U is strongly correlated with PC2. Fe, Mo and Ni are also weakly correlated with PC2. At Becconsall-1Z, Fe, TiO_2, Al, K and Zr are correlated with PC1 and are inversely correlated with Ca. Ni and TOC are correlated with PC2. Mo and U are correlated with PC1 and PC2. S is correlated with PC2 and inversely correlated with PC1. At Hind Clough the variance is more complex; PC1 and PC2 represent less than half of the total variance in the dataset. Zr, TiO_2 and Al are correlated with PC1. Mo is strongly correlated with PC2.

TOC is inversely correlated with PC1 and correlated with PC2. Fe, Ni, S and U are inversely correlated with PC2.

Finally, we plotted the traditional biplots of Mo-EF versus U-EF and Mo versus TOC with the fields of Tribovillard *et al*. (2012) and Algeo and Lyons (2006) (**Fig. 6**). The modern seawater (SW) Mo/U ratio defined in Algeo and Tribovillard (2009) are also plotted for comparison. The correlation coefficients between Mo and TOC concentrations vary between the three sites. At Becconsall-1Z, Mo and TOC are not correlated (R^2 of 0.18). Mo and TOC are weakly correlated at Preese Hall-1 (R^2 of 0.47). At Hind Clough, the correlation coefficient between Mo and TOC is 0.59 (moderate correlation).

Rock-Eval(6) Pyrolysis

TOC concentrations are wide ranging at Preese Hall-1 (0.4 to 5.3 %), but Preese Hall-1 also exhibits the lowest average TOC content (2.4 %). Hind Clough and Becconsall-1Z share similar average TOC contents (3.4 %), however, their ranges differ. Hind Clough TOC values range from 1.1 to 5.0 %, whereas Beconsall-1Z range from 2.4 to 4.5 %. We used T_{max} as an indicator of organic matter thermal maturity at Preese Hall-1 (448 to 564 °C), Becconsall-1Z (454 to 469 °C) and Hind Clough (426 to 455 °C). The pyrolysis S2 yields are <11 mg/g at Hind Clough and <4.15 mg/g at Preese Hall-1 and Becconsall-1Z. TOC_0 estimates range from 0.6 to 8.3 % in Preese Hall-1, with an average of 3.8 ±1.3 %. The range in upper bound TOC_0 is largest in Preese Hall-1 and smallest at Becconsall-1Z where minimum and maximum values are 3.8 and 7.1%, and average TOC_0 is 5.3 ±0.6%. Upper bound TOC_0 estimates are largest at Hind Clough (5.4 ±0.9 %), ranging from 3.8 to 7.1 %.

Discussion

Depositional processes and provenance interpretations

This study shows how the Upper Bowland Shale varies in thickness across the Bowland sub-basin (**Fig. 2**). Controlling for temporal variation, our study shows lateral variation in the thickness of the Bowland Shale is notable and is therefore potentially difficult to predict. For example, the study succession at Preese Hall-1 is up to five and six times thicker than the same time-equivalent succession at Hind Clough (102 m thick) and Becconsall-1Z (85 m), respectively (**Fig. 2**). Emmings *et al.* (2020) showed that the sediments at Hind Clough, although more proximal than Becconsall-1Z and Preese Hall-1 shown in this study, were deposited in a relatively deep and confined area of the Bowland sub-basin. This interpretation implicates protracted sediment bypass at Hind Clough as an explanation for accumulation of the 512 m thick package at Preese Hall-1. Thus, our study highlights the importance of complex palaeobathymetry as a control on sediment routing and the development of localised depocentres. Options available for shale gas exploration via directional drilling may be more preferable towards the central Bowland sub-basin.

Gamma ray spectroscopy was used to place our observations in a wider context (i.e., upscale to the well scale). The Upper Bowland Shale was only partially cored at Becconsall-1Z and Preese Hall-1. Therefore, comparisons of palaeoceanographic changes throughout the entire formation are not currently possible. However, both gamma ray logs from Preese Hall-1 and Becconsall-1Z are consistently serrated (saw-tooth) and aggrading, which supports the extrapolation of the discrete geochemical observations in this current study to a larger scale. There are, for example, no major or consistent changes in the gamma ray logs or mineralogy within the cores at Preese Hall-1 or

Becconsall-1Z which might have otherwise affected our interpretation of provenance and early diagenesis.

The geochemical provenance proxies support the established sedimentological regional interpretations of a primary felsic igneous, intermediate igneous and/or quartzose sedimentary origin (**Table 1** and **Fig. 3**). Cross-plots of TiO_2 versus Zr, as well as TiO_2 versus Ni, are consistent with the interpretation that the Upper Bowland Shale is of a northern sandstone-derived origin (Gilligan 1920; Reading 1964; Drewery *et al.* 1987; Lawrence *et al.* 1987; Collinson *et al.* 1988; Leeder 1988; Cliff *et al.* 1991; Clarke *et al.* 2018), and more similar in composition to felsic igneous rocks. The TiO_2-Zr biplot suggests that Upper Bowland Shale sediments share a similar provenance at each site. Hind Clough is potentially more mature in terms of sediment provenance; this may be explained by sediment fractionation within the sub-basin.

It has been previously suggested that Ni is an indicator proxy for provenance (Floyd *et al.* 1989), however Ni is also redox-sensitive (Tribovillard *et al.* 2006) and enrichment and depletion in the Bowland Shale is linked to the position of the redoxclines (Emmings *et al.* 2020a). In **Fig. 3**, relative low values of TiO_2 at all 3 sites (0.69 and 0.05 %) suggest that despite the addition of autochthonous Ni under sulfidic conditions, it is possible to infer a felsic (rather than mafic) sedimentary provenance of the Upper Bowland Shale. Other provenance proxies were not used (e.g. discriminant function plots of Roser and Korsch 1988) because the extreme maximum burial depth of the Upper Bowland Shale, inferred from vitrinite reflectance, reached *c.* 130°C (e.g., Clarke *et al.* 2018). This would likely minimise the effectiveness of provenance interpretation for some elements, for example due to the diagenetic mobility of K (Wintsch and Kvale 1994).

Palaeoredox interpretations

Here we interpret palaeoredox conditions within a time-equivalent interval bounded by the biostratigraphic markers $E_{1a}1$ and $E_{1b}2$ (**Fig. 2**). To build confidence in the interpretation of U-EF and Mo-EF in terms of palaeoredox conditions, we first compared U-EF and Mo-EF to the concentrations of Zr and TiO_2, elements which proxy for detrital provenance (see prior discussion) **(Fig. 4)**. In all three sections, U-EF and Mo-EF do not correlate or covary with Zr or TiO_2. This shows sediment fractionation and dilution effects, including unusual enrichment in Mo and U in the detrital sand-bearing component are not credible controls on Mo-EF and U-EF. Therefore, we are confident that the abundances of Mo and U, and their enrichment factors, are strongly influenced by the anoxic and/or euxinic bottom water redox conditions.

U-EF and Mo-EF are not generally correlated with TOC; it is therefore not possible to directly interpret TOC simplistically in terms of changes in bottom water redox conditions. TOC in Becconsall-1Z is most strongly coupled to redox conditions based on relatively strong correlation between TOC and U-EF **(Fig. 4)** and strong correlation between Ni and TOC (and to a lesser degree U and Mo) using PCA **(Fig. 5)**. This may indicate an increased fraction of autochthonous organic matter deposited at Becconsall-1Z, associated with tighter coupling between organic matter input and preservation, and the development of sulfidic porewaters. At Preese Hall-1 and Hind Clough the controls on TOC are more complex, and likely involve factors such as sediment dilution and autodilution (e.g., radiolarian silica, skeletal carbonate), sediment reworking, redox oscillation, mobility during diagenesis and catagenesis, and a mixture of different types of organic matter (autochthonous, allochthonous).

The biplots of U-EF and Mo-EF indicate all samples between the $E_{1a}1$ and $E_{1b}2$ marine bands were deposited under anoxic and at least intermittently sulfidic bottom water conditions (**Fig. 6**). Relatively high Mo-EF compared to U-EF suggests operation of moderate to strong Fe-Mn particulate shuttle. Mo compared to the present-day TOC (and our upper bound estimate for TOC_0) suggests bottom water anoxia in the Bowland sub-basin was likely weakly to moderately restricted **(Fig. 6).** This equates to deep-water renewal times of ca. 10-1000 years, also found in the modern Cariaco Basin and Framvaren Fjord (Algeo and Lyons, 2006). A small number samples with very low Mo/TOC_0 potentially indicates intermittent development of highly restricted bottom water conditions.

Overall, these interpretations are broadly consistent with the proposed, weakly restricted, productive model for water column conditions in the proximal Craven Basin (Emmings *et al.* 2020). Based on our new observations, concurrent anoxia developed at the margins and centre of the Bowland sub-basin. We thus extend the interpretation of Emmings *et al*. (2020) from the proximal (Hind Clough) to the distal settings of the Bowland sub-basin. The interpretation of basin-wide anoxia is comparable to interpretations from broadly time-equivalent packages in other basins. For example, Riley *et al*. (2016) and Gross *et al*. (2015) demonstrated development of Upper Bowland-Hodder anoxia in the Gainsborough Trough and in the Widermerpool Gulf, respectively. Emmings *et al*. (this volume) shows development of intermittent anoxia in the Blacon Basin. Therefore it is clear anoxia developed at least intermittently in multiple adjacent basins during deposition of the Bowland Shale, and was therefore likely regional in scale (Parnell *et al.* 2016) (Sims *et al*., this volume). It is plausible that Bowland sub-basin anoxia was productivity-driven, particularly at Becconnsall-1Z; future work should investigate the link between the preservation of labile organic matter and anoxia in the Bowland sub-basin.

The bottom-water conditions of the Bowland sub-basin (Upper Bowland Shale) apparently favoured organic carbon preservation during deposition and early-stage diagenesis, which resulted in present day average TOC contents of 3.4 % in Becconsall-1Z and 2.4 % in Preese Hall-1 (averages exceed 2 % in each well). Present day TOC contents >2% are often used as a criterion for viable unconventional hydrocarbon extraction (e.g., Andrews, 2013). The present day TOC values at Becconsall-1Z and in Preese Hall-1 are high, considering the elevated thermal maturity. If hydrocarbon exploration should proceed in the Bowland sub-basin, directional drilling could target the north and/or central Bowland sub-basin, where the Upper Bowland Shale is up to 6 times thicker than at the sub-basin margin and average TOC and TOC_0 values exceed 2 %. Furthermore, exploration in the thicker succession (towards the centre of this sub-basin) could provide more core material for laterally applicable sweet spot identification. However, previous authors (Hennissen *et al.* 2017; Emmings *et al.* 2020) have advised caution in the use of bulk present-day TOC data as a criterion for sweet spot analysis following their investigations in the proximal part of the Craven Basin and in the Widmerpool Gulf (in immature to light oil mature sections) which contain a large fraction of thermally refractory carbon (up to 80%).

Is the Barnett Shale Formation a suitable analogue?

The Barnett Shale Formation has been used previously (Andrews 2013; Whitelaw *et al.* 2019) as an analogue to the Bowland Shale Formation. Andrews (2013) developed gas-in-place estimates for the Bowland Shale on the basis that these two formations were a suitable comparison. However, we suggest that the Barnett Shale Formation is not a suitable analogue for Bowland Shale Formation for several reasons. Firstly, the Bowland Shale exhibits structural complexity, fracturing, faulting, and

compartmentalisation at the sub-basin to basin scale (e.g., Anderson and Underhill 2020; Anderson *et al.* 2022). By contrast, the Barnett Shale is relatively uniform at the basin scale (e.g., Fort Worth Basin) and is less compartmentalized (e.g., Loucks and Ruppel 2007). The Upper Bowland Shale was deposited under a high mean sediment accumulation rate, up to an order of magnitude faster than the Barnett Shale after accounting for duration of deposition (Emmings *et al.* 2020a). Marine bands in the Bowland Shale are typically carbonate cemented and the formation is typically siliceous, but it also contains a significant fraction of detrital clay supplied from the Pendle delta system, particularly in the Upper Bowland Shale (e.g., Emmings *et al.* 2020a).

Finally, we show that the formations differ in terms of palaeoceanographic restriction (e.g., **Fig. 6**). Anoxia during deposition of Barnett Shale developed in a moderately to highly restricted basin and was coupled to third-order sea level cyclicity (Rowe *et al.* 2008; Gambacorta *et al.* 2016). This contrasts with anoxia in the Bowland Shale which likely developed under productive, nutrient-rich water column conditions, in a weakly to moderately restricted basin, modulated by *fourth-order* sea level cyclicity, fed by major prograding delta systems, and subject to a moderate to strong Fe-Mn (oxyhydr)oxide shuttle. Thus, anoxia during deposition of the Barnett Shale was comparatively long-lived (third order sea level fluctuation) and potentially associated with development of relatively stable chemoclines. This is consistent with a lack of evidence for Fe-Mn (oxyhydr)oxide shuttling in the Barnett Shale (Gambacorta *et al*. 2016). These differences are inextricably linked to the regional structural complexity and proximity to major delta systems.

A key consequence in terms of hydrocarbon prospectivity is understanding the pathways of organic matter preservation, which in turn impacts on the spatiotemporal *predictability* in key rock properties for unconventional hydrocarbon extraction. Weakly to moderately restricted, Fe-Mn (oxyhydr)oxide rich, productivity-driven, prodeltaic basins potentially represent more unstable and transient systems, and are associated with strong lateral variation in syngenetic and early diagenetic conditions, including potential for redox oscillation under anoxic conditions (Emmings *et al*. 2020 Palaeo-3). Such conditions are more likely to promote organic matter degradation and recycling in the water column through processes such as 'priming' or co-oxidation (e.g., Aller 1994). We suggest this phenomenon may explain, at least in part, why the Bowland Shale TOC comprises a low proportion of pyrolysable carbon, even in low thermal maturity sections (e.g., Hennissen *et al*. 2017, Emmings et al. 2020) which nonetheless can contain a relatively large proportion of autochthonous marine organic matter. Understanding the fraction of pyrolizable organic matter is also critically important to the accurate derivation of TOC_0 – and by extension - the way we interpret Mo/TOC_o as a proxy for water column restriction (e.g., Hart and Hofmann 2022). Further work should investigate the potentially contrasting pathways of organic matter preservation in the Bowland and Barnett shales, which may represent end-members.

Conclusions

(1) The geochemistry (e.g., Zr, TiO2, Ni) and sedimentology to show the Upper Bowland Shale was sourced from a quartzo-feldspathic primary provenance; indicative of a felsic igneous, intermediate and/or quartzose sedimentary provenance.

(2) Assessment of the redox proxies Mo and U suggests anoxia in the Upper Bowland Shale developed under weakly restricted conditions,

consistent with prior observations in the proximal Bowland sub-basin and from other adjacent basins.

(3) The relative increase in maximum TOC and TOC_0 towards the central Bowland sub-basin reflects a likely increase in hydrocarbon potential towards Preese Hall-1. Additionally, the sedimentary package at Preese Hall-1 is thicker, relative to Becconsall-1Z, suggesting that the central Bowland sub-basin may be a more favourable shale gas target than the southern part of the sub-basin.

(4) A comparison of the depositional palaeoceanography of the Bowland sub-basin and Fort Worth Basin (Mississippian Barnett Shale) shows that Fort Worth Basin was more restricted than the Bowland sub-basin. Overall, we conclude the Barnett Shale is not a strong analogue for the Bowland Shale based on considerations of basin structure, depositional and early diagenetic redox processes, and present-day bulk composition.

Acknowledgements

This project was funded by the NERC Oil and Gas Centre for Doctoral Training Programme, Newcastle University, and the British Geological Survey - University Funding Initiative (BUFI).

CH Vane, JAI Hennissen and E Hough publish with the permission of the Executive Director of the British Geological Survey (BGS-UKRI).

Author Contributions (CRediT Taxonomy):

JW: conceptualisation (lead), data curation (lead), formal analysis (lead), investigation (lead), methodology (equal), original draft (lead), writing – review and editing (lead). **JFE:** conceptualisation (lead), data curation (lead), formal analysis (lead), investigation (lead), methodology (equal), original draft (supporting), writing – review and editing (supporting). **SA:** conceptualisation (supporting), data curation (supporting), formal analysis (supporting), investigation (supporting), methodology (equal), original draft (supporting), writing – review and editing (supporting). **SLF:** conceptualisation (supporting), data curation (supporting), formal analysis (supporting), investigation (supporting), methodology (equal), original draft (supporting), writing – review and editing (supporting). **CVDL:** conceptualisation (supporting), data curation (supporting), formal analysis (supporting), investigation (supporting), methodology (equal), original draft (supporting), writing – review and editing (supporting). **MJ:** conceptualisation (supporting), data curation (supporting), formal analysis (supporting), investigation (supporting), methodology (equal), original draft (supporting), writing – review and editing (supporting). **CHV:** conceptualisation (supporting), data curation (supporting), formal analysis (supporting), investigation (supporting), methodology (equal), original draft (supporting), writing – review and editing (supporting). **JAIH:** conceptualisation (supporting), data curation (supporting), formal analysis (supporting), investigation (supporting), methodology (equal), original draft (supporting), writing – review and editing (supporting). **EH:** conceptualisation (supporting), data curation (supporting), formal analysis (supporting), investigation (supporting), methodology (equal), original draft (supporting), writing – review and editing (supporting). **TW:** conceptualisation (supporting), data curation (supporting), formal analysis (supporting), investigation (supporting), methodology (equal), original draft (supporting), writing – review and editing (supporting). **LC:** conceptualisation (supporting), data curation (supporting), formal analysis (supporting), investigation (supporting), methodology (supporting), original draft (supporting), writing – review and editing (supporting)

References

Aitkenhead, N. 1992. Geology of the Country Around Garstang: Memoir for 1: 50,000 Geological Sheet 67 (England and Wales). HM Stationery Office.

Algeo, T.J., Lyons, T.W., Blakey, R.C. and Over, D.J., 2007. Hydrographic conditions of the Devono–Carboniferous North American Seaway inferred from sedimentary Mo–TOC relationships. *Palaeogeography, Palaeoclimatology, Palaeoecology*, *256*(3-4), pp.204-230.

Algeo, T.J. and Lyons, T.W., 2006. Mo–total organic carbon covariation in modern anoxic marine environments: Implications for analysis of paleoredox and paleohydrographic conditions. *Paleoceanography*, *21*(1).

Algeo, T.J. and Tribovillard, N. 2009. Environmental analysis of paleoceanographic systems based on molybdenum–uranium covariation. Chemical Geology, **268**, 211-225.

Aller, R.C., 1994. Bioturbation and remineralization of sedimentary organic matter: effects of redox oscillation. *Chemical Geology*, *114*(3-4), pp.331-345.

Andrews, I.J. 2013. The Carboniferous Bowland Shale gas study: geology and resource estimation.

de Jonge-Anderson, I. and Underhill, J.R., 2020. Structural constraints on Lower Carboniferous shale gas exploration in the Craven Basin, NW England. *Petroleum Geoscience*, *26*(2), pp.303-324.

de Jonge-Anderson, I., Hollinsworth, A.D., Underhill, J.R. and Jamieson, R.J., 2022. A geological assessment of the carbon storage potential of structural closures in the East Midlands shelf, United Kingdom Southern North Sea. *AAPG Bulletin*, *106*(9), pp.1827-1853.

Arthurton, R.S. 1984. The Ribblesdale fold belt, NW England—a Dinantian-early Namurian dextral shear zone. Geological Society, London, Special Publications, **14**, 131-138.

Arthurton, R.S., Johnson, E.W. and Mundy, D. 1988. Geology of the country around Settle.

Baptie, B.J., Segou, M., Hough, E., Hennissen, J.A.I., 2022. Recent scientific advances in the understanding of induced seismicity from hydraulic fracturing of shales, British Geological Survey, Keyworth, Nottingham, United Kingdom, pp. 51. https://www.gov.uk/government/publications/review-of-the-geological-science-of-shale-gas-fracturing

Beck, M., Dellwig, O., Schnetger, B. and Brumsack, H.-J. 2008. Cycling of trace metals (Mn, Fe, Mo, U, V, Cr) in deep pore waters of intertidal flat sediments. Geochimica et Cosmochimica Acta, **72**, 2822-2840.

Behar, F., Beaumont, V. and Penteado, H.D.B. 2001. Rock-Eval 6 technology: performances and developments. Oil & Gas Science and Technology, **56**, 111-134.

Bhattacharya, J.P. 1993. The expression and interpretation of marine flooding surfaces and erosional surfaces in core; examples from the Upper Cretaceous Dunvegan Formation, Alberta foreland basin, Canada. Sequence stratigraphy and facies associations, 125-160.

Bisat, W.S. 1922. Yorkshire Naturalists at Clitheroe. Naturalist, 225-226.

Bisat, W.S. 1924. The Carboniferous Ammonoids of the North of England and their zones. Yorkshire Geological Society, **20**, 40-124.

Brandon, A. 1998. Geology of the Country Around Lancaster: Memoir for 1: 50 000 Geological Sheet 59 (England and Wales). Stationery Office.

Brumsack, H.-J. 2006. The trace metal content of recent organic carbon-rich sediments: implications for Cretaceous black shale formation. Palaeogeography, Palaeoclimatology, Palaeoecology, **232**, 344-361.

Church, K.D. and Gawthorpe, R.L. 1994. High resolution sequence stratigraphy of the late Namurian in the Widmerpool Gulf (East Midlands, UK). Marine and Petroleum Geology, **11**, 528-544.

Clarke, H., Turner, P., Bustin, R.M., Riley, N. and Besly, B. 2018. Shale gas resources of the Bowland Basin, NW England: a holistic study. Petroleum Geoscience, **24**, 287-322.

Cliff, R., Drewery, S. and Leeder, M. 1991. Sourcelands for the Carboniferous Pennine river system: constraints from sedimentary evidence and U-Pb geochronology using zircon and monazite. Geological Society, London, Special Publications, **57**, 137-159.

Cocks, L. and Torsvik, T. 2006. European geography in a global context from the Vendian to the end of the Palaeozoic. MEMOIRS-GEOLOGICAL SOCIETY OF LONDON, **32**, 83.

Collinson, J.D. 1968. Deltaic sedimentation units in the Upper Carboniferous of northern England. Sedimentology, **10**, 233-254.

Collinson, J.D. 1969. The sedimentology of the Grindslow Shales and the Kinderscout Grit: a deltaic complex in the Namurian of northern England. Journal of Sedimentary Research, **39**.

Collinson, J.D., Besly, B.M. and Kelling, G. 1988. Controls on Namurian sedimentation in the Central Province basins of northern England. Sedimentation in a synorogenic basin complex: the Upper Carboniferous of Northwest Europe. Blackie, Glasgow, **85**, 101.

Corfield, S., Gawthorpe, R., Gage, M., Fraser, A. and Besly, B. 1996. Inversion tectonics of the Variscan foreland of the British Isles. Journal of the Geological Society, **153**, 17-32.

Craigie, N.W., 2018. Principles of elemental chemostratigraphy. Advances in Oil and Gas Exploration & Production, Rudy Swennen. A Practical User Guide. p189. DOI: https://doi. org/10.1007/978-3-319-71216-1.

Craigie, N.W. 2015. Applications of chemostratigraphy in Middle Jurassic unconventional reservoirs in eastern Saudi Arabia. GeoArabia, **20**, 79-110.

Davies, S. and McLean, D. 1996. Spectral gamma-ray and palynological characterization of Kinderscoutian marine bands in the Namurian of the Pennine Basin. Proceedings of the Yorkshire Geological Society, **51**, 103-114.

Davies, S. and Elliott, T. 1996. Spectral gamma ray characterization of high resolution sequence stratigraphy: examples from Upper Carboniferous fluvio-deltaic systems, County Clare, Ireland. Geological Society, London, Special Publications, **104**, 25-35.

Davies, S., Guion, P. and Gutteridge, P. 2012. Carboniferous sedimentation and volcanism on the Laurussian margin. Geological history of Britain and Ireland, 231-273.

Drewery, S., Cliff, R. and Leeder, M. 1987. Provenance of Carboniferous sandstones from U–Pb dating of detrital zircons. Nature, **325**, 50.

Dunham, K.C. and Wilson, A.A. 1985. Geology of the Northern Pennine oilfield: Volume 2 Stainmore to Craven.

Earp, J., Poole, E.G. and Whiteman, A. 1961. Geology of the country around Clitheroe and Nelson. HM Stationery Office.

Ellis, D.V. and Singer, J.M. 2007. Well logging for earth scientists. Springer.

Emmings, J.F., Davies, S.J., Vane, C.H., Moss-Hayes, V. and Stephenson, M.H. 2020a. From marine bands to hybrid flows: Sedimentology of a Mississippian black shale. Sedimentology, **67**, 261-304.

Emmings, J.F., Dowey, P.J., Taylor, K.G., Davies, S.J., Vane, C.H., Moss-Hayes, V. and Rushton, J.C. 2020b. Origin and implications of early diagenetic quartz in the Mississippian Bowland Shale Formation, Craven Basin, UK. Marine and Petroleum Geology, **120**, 104567.

Emmings, J.F., Hennissen, J.A. et al. 2019. Controls on amorphous organic matter type and sulphurization in a Mississippian black shale. Review of Palaeobotany and Palynology, **268**, 1-18.

Emmings, J.F., Davies, S.J., Vane, C.H., Leng, M.J., Moss-Hayes, V., Stephenson, M.H. and Jenkin, G.R., 2017. Stream and slope weathering effects on organic-rich mudstone geochemistry and implications for hydrocarbon source rock assessment: A Bowland Shale case study. *Chemical Geology*, *471*, pp.74-91.

Fewtrell, M.D., Smith, D.G., Clayton, G. and Sevastopulo, G.D. 1981. Discussion on the recognition and division of the Tournaisian Series in Britian. Journal of the Geological Society, London, **137**, 61-63.

Fearn, G., 2022. The age of the manager is over? Shale gas fracking and the challenge to the post-political regime for English planning. Political Geography, 93, p.102550.

Floyd, P., Winchester, J. and Park, R. 1989. Geochemistry and tectonic setting of Lewisian clastic metasediments from the Early Proterozoic Loch Maree Group of Gairloch, NW Scotland. Precambrian Research, **45**, 203-214.

Fraser, A.J., Nash, D.F., Steele, R.P., Ebdon, C.C. and Fraser, A.J., 1990. A regional assessment of the intra-Carboniferous play of Northern England. *Geological Society, London, Special Publications*, *50*(1), pp.417-440.

Fraser, A.J. and Gawthorpe, R. 1990. Tectono-stratigraphic development and hydrocarbon habitat of the Carboniferous in northern England. Geological Society, London, Special Publications, **55**, 49-86.

Fraser, A.J. and Gawthorpe, R.L. 2003. An atlas of Carboniferous basin evolution in northern England.

Gambacorta, G., Trincianti, E. and Torricelli, S., 2016. Anoxia controlled by relative sea-level changes: An example from the Mississippian Barnett Shale Formation. Palaeogeography, Palaeoclimatology, Palaeoecology, 459, pp.306-320.

Gawthorpe, R. 1987. Tectono-sedimentary evolution of the Bowland Basin, N England, during the Dinantian. Journal of the Geological Society, **144**, 59-71.

Gilligan, A. 1920. The petrography of the Millstone Grit of Yorkshire. Quart. Jour. Geol. Soc. London, **70**, 251-294.

Gross, D., Sachsenhofer, R., Bechtel, A., Pytlak, L., Rupprecht, B. and Wegerer, E. 2015. Organic geochemistry of Mississippian shales (Bowland Shale Formation) in central Britain: Implications for depositional environment, source rock and gas shale potential. Marine and Petroleum Geology, **59**, 1-21.

Hampson, G.J., Elliott, T. and Davies, S.J. 1997. The application of sequence stratigraphy to Upper Carboniferous fluvio-deltaic strata of the onshore UK and Ireland: implications for the southern North Sea. Journal of the Geological Society, **154**, 719-733.

Hart, B.S. and Hofmann, M.H., 2022. Revisiting paleoenvironmental analyses and interpretations of organic-rich deposits: The importance of TOC corrections. *Organic Geochemistry*, *170*, p.104434.

Hayashi, K.-I., Fujisawa, H., Holland, H.D. and Ohmoto, H. 1997. Geochemistry of ~ 1.9 Ga sedimentary rocks from northeastern Labrador, Canada. Geochimica et cosmochimica acta, **61**, 4115-4137.

Hennissen, J.A. and Montesi, G., 2020. Quantitative palynological analysis of the E2a and E2b ammonoid biozones (Arnsbergian, Mississippian) in mudstones from the Southern Pennine Basin (UK). *Review of Palaeobotany and Palynology*, *276*, p.104187.

Hennissen, J.A. and Gent, C.M. 2019. Total organic carbon in the Upper Bowland Shale of the southern Widmerpool Gulf: a discussion. Journal of Petroleum Science and Engineering, **178**, 1194-1202.

Hennissen, J.A.I., Hough, E., Vane, C.H., Leng, M.J., Kemp, S.J. and Stephenson, M.H. 2017. The prospectivity of a potential shale gas play: An example from the southern Pennine Basin (central England, UK). Marine and Petroleum Geology, **86**, 1047-1066, https://doi.org/https://doi.org/10.1016/j.marpetgeo.2017.06.033.

Henry, D.G., Jarvis, I., Gillmore, G., Stephenson, M. and Emmings, J.F., 2018. Assessing low-maturity organic matter in shales using Raman spectroscopy: Effects of sample preparation and operating procedure. *International Journal of Coal Geology*, *191*, pp.135-151.

Hird, C., Clarke, H. and Wood, T. 2012a. Becconsall-1 End Of Well Report. Cuadrilla Resources.

Hird, C., Clarke, H. and Turner, P. 2012b. Preese Hall 1A End of Well Report. LJ/06-5 (End of Well Report). Cuadrilla Resources.

Holdsworth, B. and Collinson, J. 1988. Millstone Grit cyclicity revisited. Sedimentation in a synorogenic basin complex. The Upper Carboniferous of Northwest Europe, 132-152.

HOLMES, D.T. & BUHR, K.A. 2007. Error propagation in calculated ratios. Clinical biochemistry, **40**, 728-734.

Horn, M. 1960. Die Zone des Eumorphoceras pseudobilingue im Sauerland. Fortschritte in der Geologie von Rheinland und Westfalen, **3**, 303-342.

Hough, E., Vane, C.H., Smith, N.J. and Moss-Hayes, V.L. 2014. The Bowland Shale in the Roosecote borehole of the Lancaster fells Sub-Basin, Craven Basin, UK: a potential UK Shale gas play? SPE/EAGE European Unconventional Resources Conference and Exhibition. European Association of Geoscientists & Engineers, 1-11.

Isbell, J.L., Miller, M.F., Wolfe, K.L. and Lenaker, P.A. 2003. Timing of late Paleozoic glaciation in Gondwana: Was glaciation responsible for the development of Northern Hemisphere cyclothems? Special papers-geological society of America, 5-24.

Jarvie, D.M., Hill, R.J., Pollastro, R.M., Wavrek, D.A., Bowker, K.A., Claxton, B.L., Tobey, M.H., 2003. Evaluation of Unconventional Natural Gas Prospects: The Barnett Shale Fractured Shale Gas Model: Poster Presented at the 21st International Meeting on Organic Geochemistry, September 8–12, Krakow, Poland.

Kane, I.A., 2010. Development and flow structures of sand injectites: The Hind Sandstone Member injectite complex, Carboniferous, UK. *Marine and Petroleum Geology*, *27*(6), pp.1200-1215.

Lawrence, S., Coster, P., Ireland, R., Brooks, J. and Glennie, K. 1987. Structural development and petroleum potential of the northern flanks of the Bowland Basin (Carboniferous), north-west England. Petroleum Geology of North West Europe. Graham and Trotman, London, **225**, 233.

Leeder, M. 1988. Recent developments in Carboniferous geology: a critical review with implications for the British Isles and NW Europe. Proceedings of the Geologists' Association, **99**, 73-100.

Lodhia, B.H., Parent, A., Fraser, A.J., Nuemaier, M., Hennissen, J.A.I., 2023. Thermal evolution and resources of the Bowland Basin (NW England) from apatite fission-track analyses and multidimensional basin modelling. Geological Society of London Special Publications.

Loucks, R.G. and Ruppel, S.C., 2007. Mississippian Barnett Shale: Lithofacies and depositional setting of a deep-water shale-gas succession in the Fort Worth Basin, Texas. *AAPG bulletin*, *91*(4), pp.579-601.

Martinsen, O. 1993. Namurian (Late Carboniferous) Depositional Systems of the Craven-Area, Northern England: Implications for Sequence-Stratigraphic Models. Sequence stratigraphy and facies associations, 247-281.

Martinsen, O.J. 1990. Fluvial, inertia-dominated deltaic deposition in the Namurian (Carboniferous) of northern England. Sedimentology, **37**, 1099-1113.

Martinsen, O.J., Collinson, J.D. and Holdsworth, B.K. 1995. Millstone Grit cyclicity revisited, II: sequence stratigraphy and sedimentary responses to changes of relative sea-level. Sedimentary Facies Analysis: A Tribute to the Research and Teaching of Harold G. Reading, 305-327.

Merriman, R.J., Kemp, S.J. 1996. Clay minerals and sedimentary basin maturity.

Montgomery, S.L., Jarvie, D.M., Bowker, K.A. and Pollastro, R.M., 2006. Mississippian Barnett Shale, Fort Worth basin, north-central Texas: Gas-shale play with multi–trillion cubic foot potential: Reply. *Aapg Bulletin*, *90*(6), pp.967-969.

Newell, A.J., Vane, C.H., Sorensen, J.P., Moss-Hayes, V. and Gooddy, D.C. 2016. Long-term Holocene groundwater fluctuations in a chalk catchment: evidence from Rock-Eval pyrolysis of riparian peats. Hydrological Processes, **30**, 4556-4567.

Noussan, M., Raimondi, P.P., Scita, R. and Hafner, M., 2020. The role of green and blue hydrogen in the energy transition—A technological and geopolitical perspective. Sustainability, 13(1), p.298.

Parnell, J., Brolly, C., Spinks, S. and Bowden, S. 2016. Selenium enrichment in Carboniferous Shales, Britain and Ireland: Problem or opportunity for shale gas extraction? Applied Geochemistry, **66**, 82-87.

Pearson, M.J. and Russell, M.A., 2000. Subsidence and erosion in the Pennine Carboniferous Basin, England: lithological and thermal constraints on maturity modelling. *Journal of the Geological Society*, *157*(2), pp.471-482.

Pharaoh, T., Haslam, R., Hough, E., Kirk, K., Leslie, G., Schofield, D. and Heafford, A., 2019. The Môn–Deemster–Ribblesdale fold–thrust belt, central UK: a concealed Variscan inversion belt located on weak Caledonian crust. *Geological Society, London, Special Publications*, *490*(1), pp.153-176.

Ramsbottom, W., Rhys, G. and Smith, E. 1962. Boreholes in the Carboniferous rocks of the Ashover district, Derbyshire. Bull. geol. Surv. Gt Br., **19**, 75-168.

Ramsbottom, W.H.C., 1977. Major cycles of transgression and regression (mesothems) in the Namurian. *Proceedings of the Yorkshire Geological Society*, *41*(3), pp.261-291.

Ramsbottom, W.H.C., MA, C., RMC, E. and DW, H. 1978. A correlation of Silesian rocks in the British Isles.

Ramsbottom, W.H.C., 1979. Rates of transgression and regression in the Carboniferous of NW Europe. *Journal of the Geological Society*, *136*(2), pp.147-153.

Ramsbottom, W.H.C. and Saunders, W.B., 1985. Evolution and evolutionary biostratigraphy of Carboniferous ammonoids. *Journal of Paleontology*, pp.123-139.

Read, J.F., Osleger, D., Elrick, M., Franseen, E.K., Watney, W.L., Kendall, C. and Ross, W. 1991. Two-dimensional modeling of carbonate ramp sequences and component cycles. Sedimentary modeling: Computer simulations and methods for improved parameter definition: Kansas Geological Survey Bulletin, **233**, 473-488.

Reading, H. 1964. A review of the factors affecting the sedimentation of the Millstone Grit (Namurian) in the Central Pennines Developments in Sedimentology. Elsevier, 340-346.

Riley, D.A., Pearce, T.J., Mathia, E., Ratcliffe, K. and Martin, J. 2016. The application of elemental geochemistry to UK onshore unconventional plays. Geological Society, London, Petroleum Geology Conference series. Geological Society of London, 585-594.

Riley, N. 1993. Dinantian (Lower Carboniferous) biostratigraphy and chronostratigraphy in the British Isles. Journal of the Geological Society, **150**, 427-446.

Roser, B.P. and Korsch, R.J. 1988. Provenance signatures of sandstone-mudstone suites determined using discriminant function analysis of major-element data. Chemical Geology, **67**, 119-139.

Rowe, H.D., Loucks, R.G., Ruppel, S.C. and Rimmer, S.M., 2008. Mississippian Barnett Formation, Fort Worth Basin, Texas: Bulk geochemical inferences and Mo–TOC constraints on the severity of hydrographic restriction. *Chemical Geology*, *257*(1-2), pp.16-25.

Scotese, C.R. and McKerrow, W.S. 1990. Revised world maps and introduction. Geological Society, London, Memoirs, **12**, 1-21.

Słowakiewicz, M., Tucker, M.E., Vane, C., Harding, R., Collins, A. and Pancost, R. 2015. Shale-gas potential of the mid-carboniferous bowland-hodder unit in the Cleveland basin (Yorkshire), central Britain. Journal of Petroleum Geology, **38**, 59-75.

Smith, N., Kirby, G. and Pharaoh, T.C. 2005. Structure and evolution of the south-west Pennine Basin and adjacent areas: subsurface memoir. British Geological Survey.

Timmerman, M.J., Heeremans, M., Kirstein, L.A., Larsen, B.T., Spencer-Dunworth, E.-A. and Sundvoll, B. 2009. Linking changes in tectonic style with magmatism in northern Europe during the late Carboniferous to latest Permian. Tectonophysics, **473**, 375-390.

Tribovillard, N., Algeo, T., Baudin, F. and Riboulleau, A. 2012. Analysis of marine environmental conditions based onmolybdenum–uranium covariation—Applications to Mesozoic paleoceanography. Chemical Geology, **324**, 46-58.

Tribovillard, N., Algeo, T.J., Lyons, T. and Riboulleau, A., 2006. Trace metals as paleoredox and paleoproductivity proxies: an update. *Chemical geology*, *232*(1-2), pp.12-32.

Van der Weijden, C.H. 2002. Pitfalls of normalization of marine geochemical data using a common divisor. Marine Geology, **184**, 167-187.

Walker, R.G. 1966. Shale Grit and Grindslow shales; transition from turbidite to shallow water sediments in the upper Carboniferous of northern England. Journal of Sedimentary Research, **36**, 90-114.

Waters, C., Waters, R., Barclay, W. and Davies, J. 2009. A lithostratigraphical framework for the Carboniferous successions of southern Great Britain (Onshore). British Geological Survey.

Waters, C.N. and Condon, D.J. 2012. Nature and timing of Late Mississippian to Mid-Pennsylvanian glacio-eustatic sea-level changes of the Pennine Basin, UK. Journal of the Geological Society, **169**, 37-51.

Wedepohl, K., Heinrichs, H. and Bridgwater, D. 1991. Chemical characteristics and genesis of the quartz-feldspathic rocks in the Archean crust of Greenland. Contributions to Mineralogy and Petrology, **107**, 163-179.

Wedepohl, K.H., Correns, C.W., Shaw, D.M., Turekian, K.K. and Zemann, J. 1969. Handbook of geochemistry.

Whitelaw, P., Uguna, C.N. et al. 2019. Shale gas reserve evaluation by laboratory pyrolysis and gas holding capacity consistent with field data. Nature communications, **10**, 1-10.

Wintsch, R.P. and Kvale, C.M. 1994. Differential mobility of elements in burial diagenesis of siliciclastic rocks. Journal of Sedimentary Research, **64**, 349-361.

Woodcock, N.H. and Strachan, R.A. 2009. Geological history of Britain and Ireland. John Wiley & Sons.

Worthington, R.P. and Walsh, J.J. 2011. Structure of Lower Carboniferous basins of NW Ireland, and its implications for structural inheritance and Cenozoic faulting. Journal of Structural Geology, **33**, 1285-1299.

Yang, S., Horsfield, B., Mahlstedt, N., Stephenson, M. and Könitzer, S. 2016. On the primary and secondary petroleum generating characteristics of the Bowland Shale, northern England. Journal of the Geological Society, **173**, 292-305.

Figure Captions

Fig. 1. (**a**) Mississippian palaeogeography of England and Wales. Major basin bounding faults typically separate extensional basins from platforms (adapted from Waters et al. 2009). BH = Bowland High; BT = Bowland Trough; CLH = Central Lancashire High; DH = Derbyshire High; EG = Edale Gulf; GT = Gainsborough Trough; LDH = Lake District High; Manx High; WG = Widmerpool Gulf. (**b**) Early Carboniferous palaeography including basins and platforms (adapted from Fraser and Gawthorpe 2003). Presence of the Permo-Triassic Cheshire Basin (Smith et al. 2005 cf.; Waters et al. 2009) and Humber Basin (Kent 1966; Hodge 2003) are controversial (Andrews 2013). (**c**) Schematic of the Visean regional basin structure including the extent of the Pendle Delta adapted from figures in Emmings et al. (2020b) and observations/interpretations from Bijkerk (2014); Fraser and Gawthorpe (2003); Fraser and Gawthorpe (1990); Waters et al. (2007) and Waters et al. (2014).

Fig. 2: Lithology of the Upper Bowland Shale across the Bowland Basin at Hind Clough, Preese Hall-1 and Becconsall-1Z (biostratigraphic markers $E_{1a}1$ and $E_{1b}2$ outlined in Hird *et al.* 2012a; 2012b).

Fig. 3: Trace metal provenance proxies for the Upper Bowland Shale using biplots of Zr versus TiO_2 (after Hayashi et al. 1997) and Ni versus TiO_2 (after Floyd et al. 1989).

Fig. 4: Biplots of uranium enrichment factors (U-EF) and molybdenum enrichment factors (Mo-EF) with TiO_2 and Zr provenance proxies, as well as TOC and maximum/minimum TOC_0.

Fig. 5: Principal Component Analyses (PCA) showing Principal Components 1 (PC1) and 2 (PC2) for geochemical proxies at Preese Hall-1, Becconsall-1Z and Hind Clough. Values used centred log-ratio (CLR) transformation. The percentage total variance (% tot. var) is displayed on each axis.

Fig. 6: Cross-plots of Mo and U trace metal enrichment factors of the Upper Bowland Shale (left) as well as Mo and TOC (and maximum/minimum TOC_0) of the Upper Bowland Shale (right) for locations Becconsall-1Z, Preese Hall-1 and Hind Clough using previous interpretations of geochemical thresholds (Algeo et al. 2007; Algeo and Tribovillard 2009; Tribovillard et al. 2012) and Barnett Shale comparisons (Rowe 2008).

Table Caption

Table 1: Geochemical data for the Upper Bowland Shale (PH-1 = Preese Hall-1; B-1Z = Becconsall-1Z; HC = Hind Clough).

									Sampling Intervals (m)		
	Proxy	**Location**		**Units**	**Average**	**Min**	**Max**	**StDev**	**Average**	**Max**	**StDev**
Whole Core	Gamma Ray (API)	PH-1		API	80.0	25.3	178.7	25.0	2.4	6.9	1.2
		B-1Z		API	112.0	26.8	238.7	45.8	0.4	1.5	0.2
	Synthetic Gamma Ray	HC			165.2	58.1	284.5	52.2	1.5	8.8	2
	XRD Cuttings	PH-1	Clay	Relative %	23.2	0.0	56.0	11.7	7.9	245.9	35.9
			Carbonate	Relative %	19.0	0.0	79.1	18.7	7.9	245.9	35.9
			Quartz	Relative %	57.8	20.9	79.0	13.1	7.9	245.9	35.9
		B-1Z	Clay	Relative %	37.7	18.0	58.6	11.9	7.5	112.3	27.9
			Carbonate	Relative %	7.5	1.8	31.0	7.2	7.5	112.3	27.9
			Quartz	Relative %	54.8	34.5	67.6	10.4	7.5	112.3	27.9
Study Succession: Base of upper Bowland Shale Formation to Top of E1b2	TiO_2	PH-1		%	0.5	0.1	0.7	0.1	1.2	3.1	1.3
		B-1Z		%	0.4	0.2	0.6	0.1	0.2	0.5	0.1
		HC		%	0.1	0.0	0.3	0.1	1.5	9.2	1.7
	Al	PH-1		%	4.7	0.6	8.9	2.0	1.2	3.1	1.3
		B-1Z		%	4.5	2.6	7.2	1.3	0.2	0.5	0.1
		HC		%	5.9	1.7	14.2	2.4	1.5	9.2	1.7
	Ni	PH-1		ppm	61.5	12.6	148.1	34.7	1.2	3.1	1.3
		B-1Z		ppm	77.5	57.1	121.1	15.3	0.2	0.5	0.1
		HC		ppm	108.6	9.8	399.4	70.1	1.5	9.2	1.7

	Mo	PH-1	ppm	19.1	1.4	59.2	14.0	1.2	3.1	1.3
		B-1Z	ppm	22.0	4.1	48.4	10.2	0.2	0.5	0.1
		HC	ppm	40.6	4.4	80.2	21.1	1.5	9.2	1.7
	Mo-EF	PH-1		37.6	2.0	83.8	18.3	1.2	3.1	1.3
		B-1Z		47.1	14.9	79.4	18.0	0.2	0.5	0.1
		HC		77.9	5.0	156.9	41.3	1.5	9.2	1.7
	U	PH-1	ppm	9.5	1.0	36.9	7.3	1.2	3.1	1.3
		B-1Z	ppm	13.0	5.1	30.6	6.4	0.2	0.5	0.1
		HC	ppm	14.4	4.6	28.9	5.6	1.5	9.2	1.7
	U-EF	PH-1		6.1	0.8	16.6	3.1	1.2	3.1	1.3
		B-1Z		8.8	4.5	16.3	3.1	0.2	0.5	0.1
		HC		8.5	4.2	20.6	3.8	1.5	9.2	1.7
	Zr	PH-1	ppm	78.1	40.9	133.1	24.3	1.2	3.1	1.3
		B-1Z	ppm	63.4	36.2	99.8	17.1	0.2	0.5	0.1
		HC	ppm	66.3	29.1	129.6	21.7	1.5	9.2	1.7
	TOC	PH-1	%	2.4	0.4	5.3	1.3	1.2	3.1	1.3
		B-1Z	%	3.4	2.4	4.5	0.6	0.2	0.5	0.1
		HC	%	3.4	1.1	5.0	0.9	1.5	9.2	1.7
	TOCo	PH-1	%	3.8	0.6	8.3	1.3	1.2	3.1	1.3
		B-1Z	%	5.3	3.8	7.1	0.6	0.2	0.5	0.1
		HC	%	5.4	1.7	7.8	0.9	1.5	9.2	1.7

Table 1

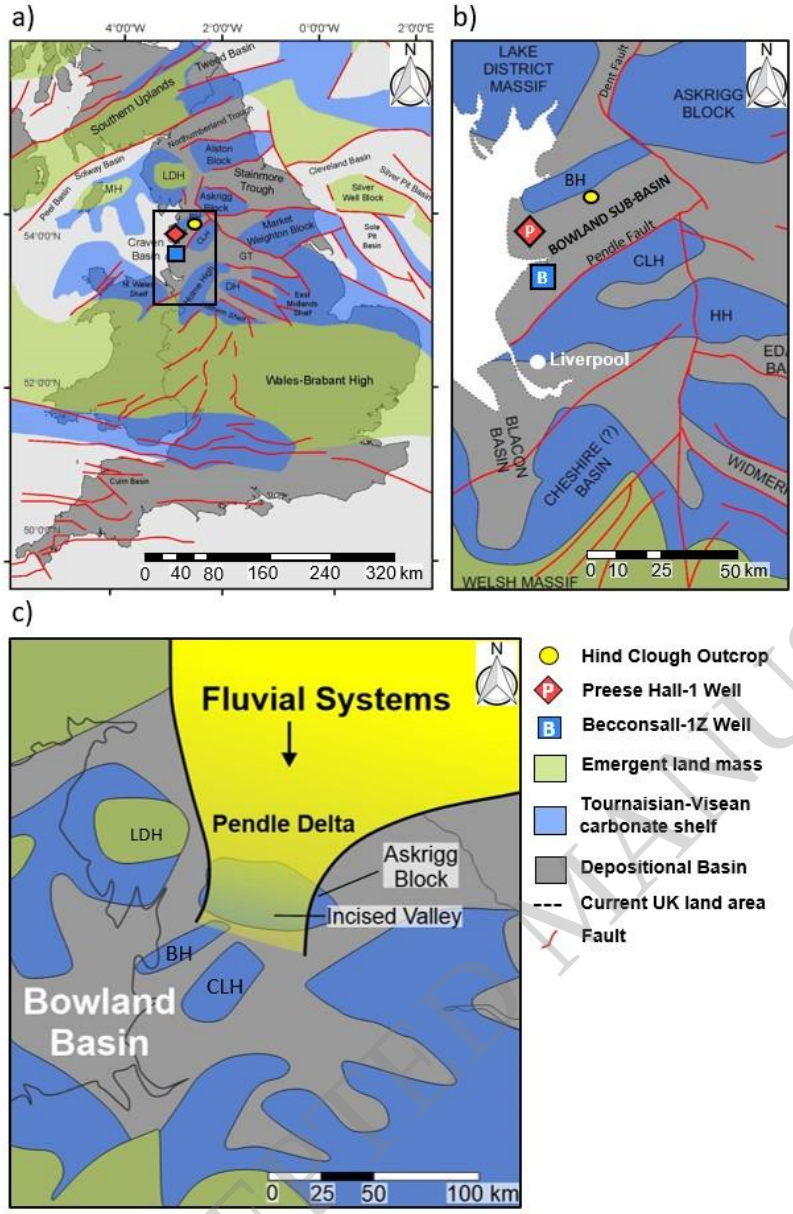

Figure 1

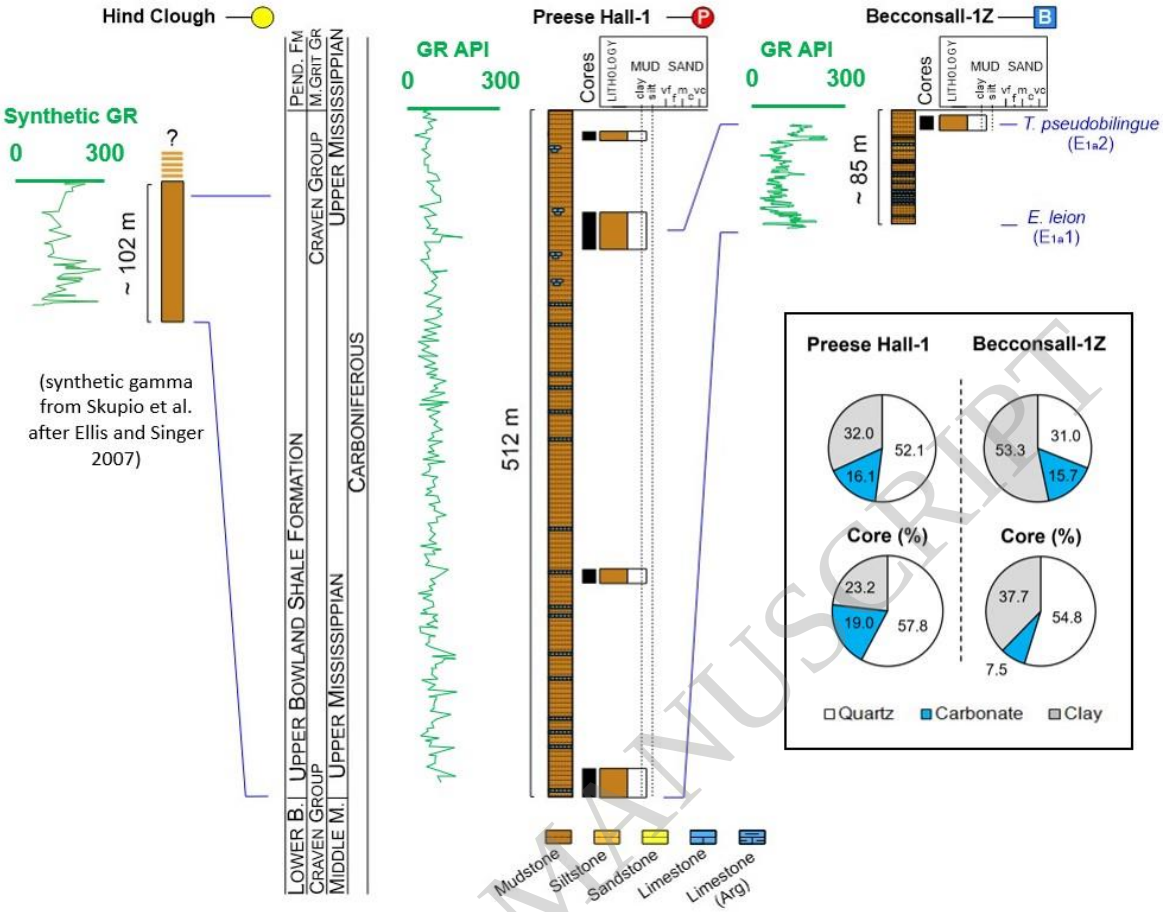

Figure 2

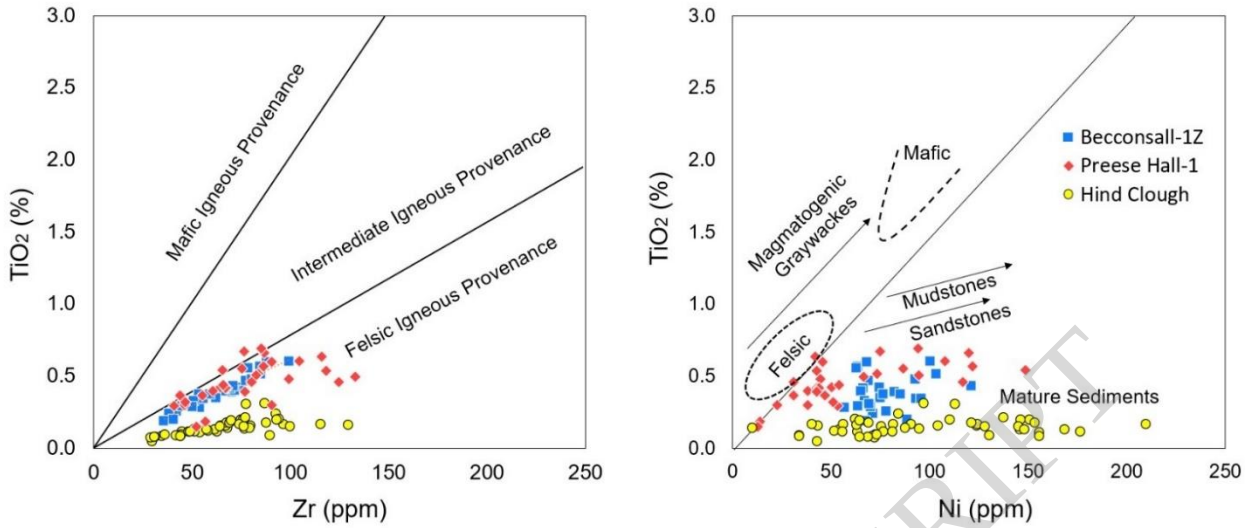

Figure 3

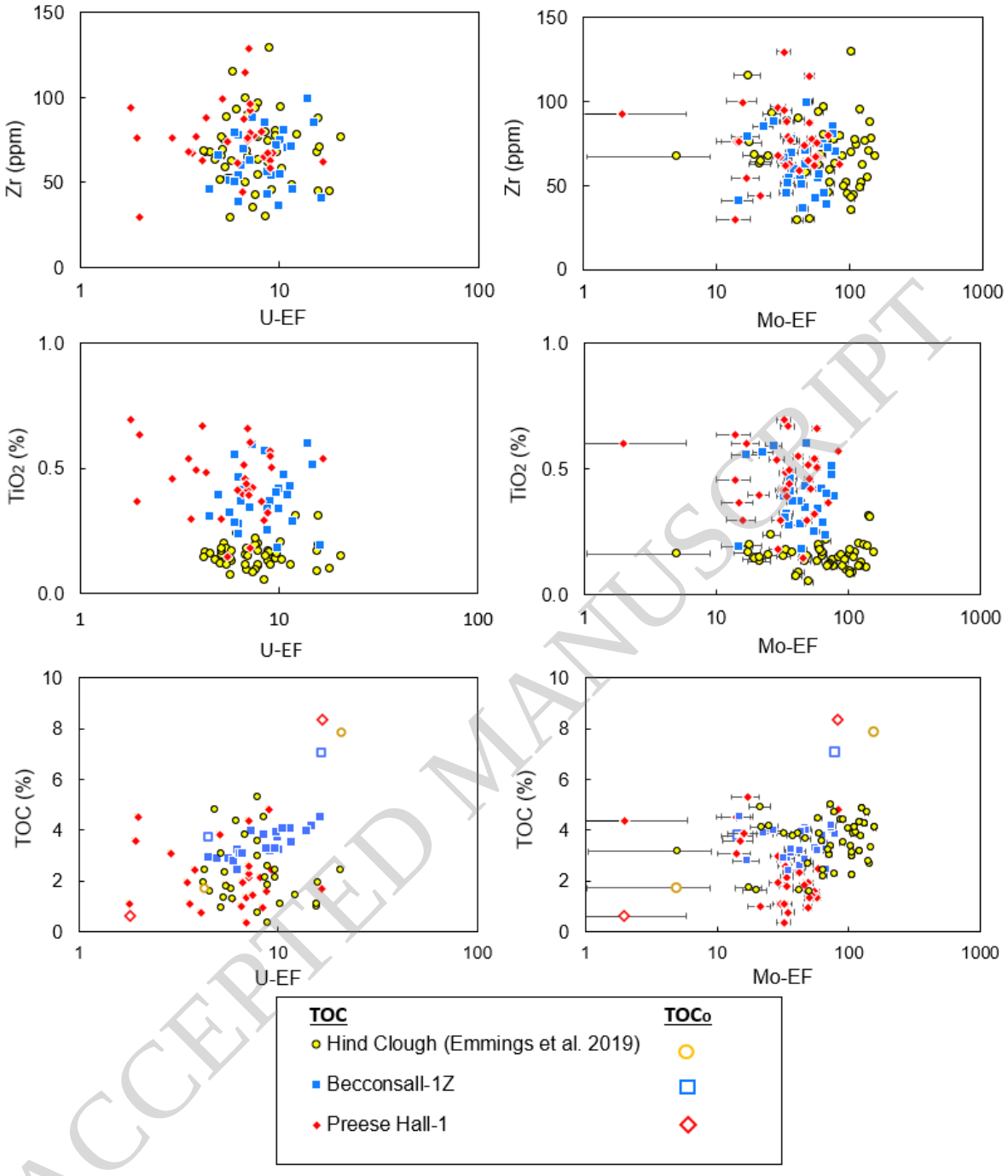

Figure 4

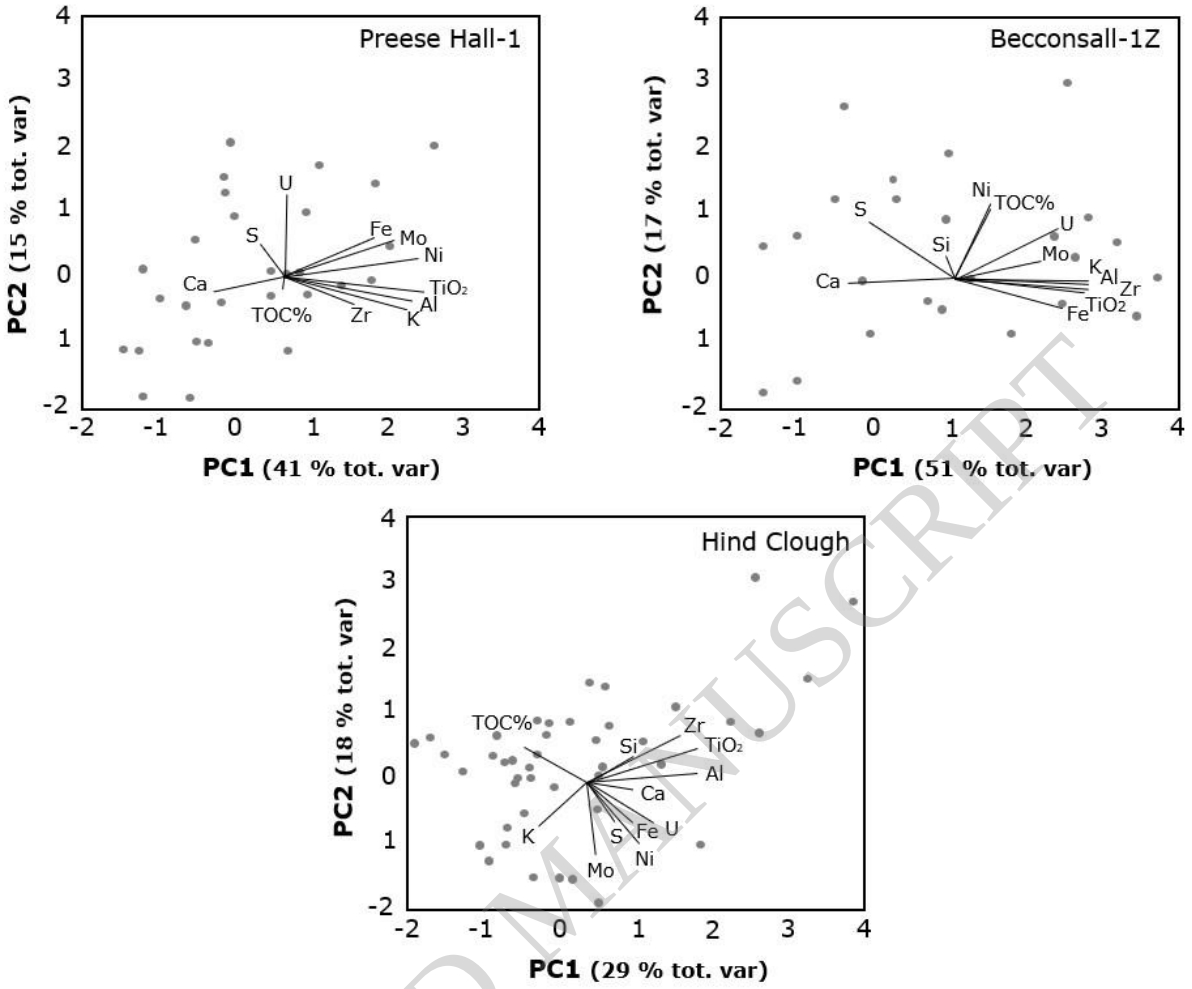

Figure 5

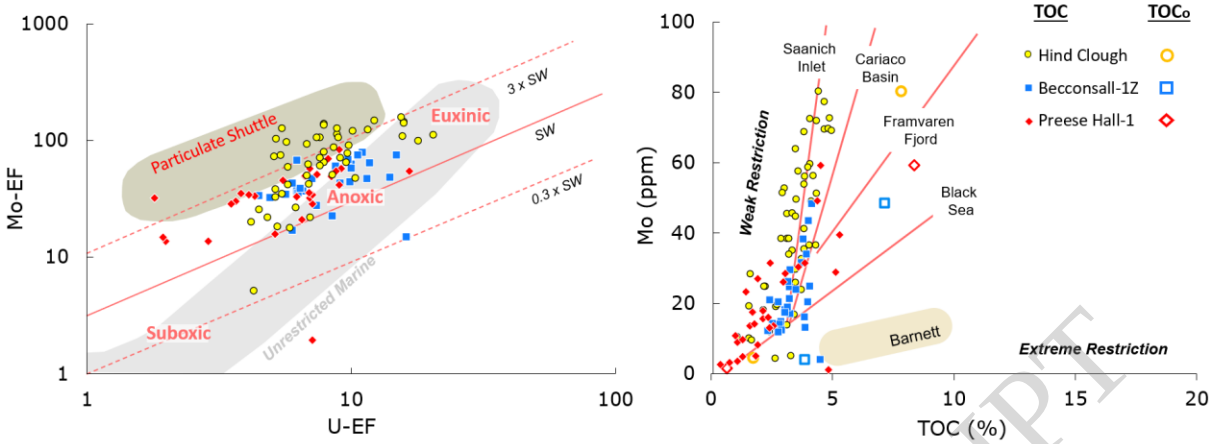

Figure 6